Available online at www.sciencedirect.com
SCIENCE DIRECT®
Earth and Planetary Science Letters 240 (2005) 425–435
EPSL
www.elsevier.com/locate/epsl

Did the Altyn Tagh fault extend beyond the Tibetan Plateau?

Brian J. Darby [a,*], Bradley D. Ritts [b,1], Yongjun Yue [c,2], Qingren Meng [d,3]

[a] Department of Geology and Geophysics, Louisiana State University, Baton Rouge, LA 70803, USA
[b] Department of Geological Sciences, Indiana University, Bloomington, IN 47405, USA
[c] Department of Geological and Environmental Sciences, Stanford University, Stanford, CA 94305-2115, USA
[d] Institute of Geology and Geophysics, Chinese Academy of Sciences, P.O. Box 9825, Beijing 100029, China

Received 3 May 2005; received in revised form 15 August 2005; accepted 13 September 2005
Available online 26 October 2005
Editor: R.D. van der Hilst

Abstract

The pre-Miocene northeastern termination of Altyn Tagh fault is a critical outstanding problem for understanding the mechanics of Cenozoic deformation resultant from the Indo-Asian collision and mechanisms of Tibetan Plateau formation. Structures beyond the widely accepted NE end of the Altyn Tagh fault, near the town of Yumen, are needed in order to accommodate strike-slip deformation related to plate-like lateral extrusion tectonics, but structures with the necessary slip magnitudes and histories have not been identified. We report on a series of newly recognized and documented E to ENE-striking faults within the Alxa block, NE of the Tibetan Plateau, that are visible on remotely sensed images and confirmed by field studies. These structures are demonstrably left-lateral faults based on offset geology and kinematic indicators such as striae and s–c fabrics in fault gouge. The faults have post-Cretaceous offsets of at least tens to possibly >150 km, but limited post-Miocene displacement, constrained by offset sedimentary basins. These characteristics suggest that strike-slip faults of the Alxa region have a similar structural history as the central-eastern Altyn Tagh fault and can provide a mechanism for accommodating Oligocene–Early Miocene extrusion along the Altyn Tagh fault.

Keywords: Altyn Tagh fault; Tibet; China; Alxa; strike-slip; tectonics

1. Introduction

The collision of India with Asia in the Early Tertiary has had profound effects on the Earth that include far-field distributed deformation and extrusion of continental blocks, inception of the Indian monsoon, changes in seawater geochemistry, and development of the world's largest and highest plateau (Fig. 1; [1–5]). Over the past 50 Ma, India has indented more than 2000 km northward into Tibet and surrounding regions [2]. The mechanisms that have accommodated strain related to India/Asia convergence within the Tibetan Plateau are highly debated but can be simplified to three basic models: continuum crustal deformation, plate-like lateral extrusion, or lower crustal flow [6–8]. These models require disparate rolls for major crustal structures such as the Karakoram fault and the Altyn Tagh fault

* Corresponding author. Tel.: +1 225 578 5810; fax: +1 225 578 2302.
Email-addresses: bdarby@geol.lsu.edu (B.J. Darby), britts@indiana.edu (B.D. Ritts), yongjun@pangea.stanford.edu (Y. Yue), qrmeng@mail.igcas.ac.cn (Q. Meng).
[1] Tel.: +1 812 856 0307; fax: +1 812 855 7899.
[2] Tel.: +1 650 723 1010; fax: +1 650 725 0979.
[3] Tel.: +86 10 62007961; fax: +86 10 64871995.

0012-821X/$ - see front matter © 2005 Elsevier B.V. All rights reserved.
doi:10.1016/j.epsl.2005.09.011

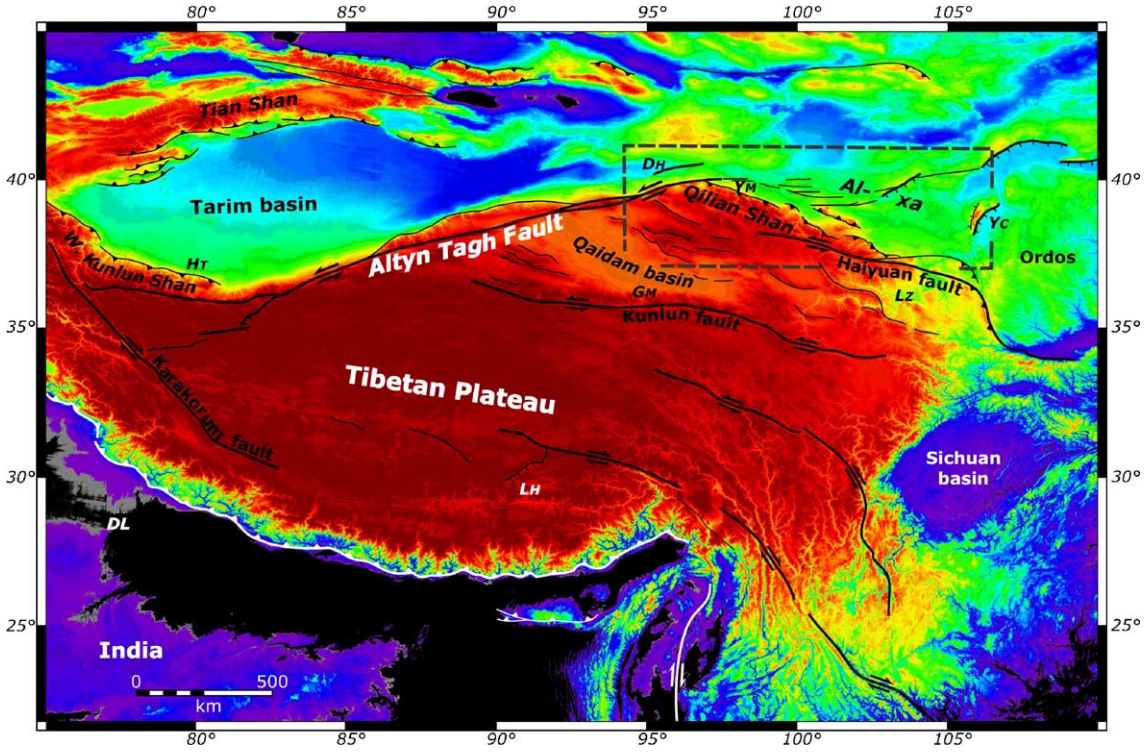

Fig. 1. Topography of the Tibetan Plateau and adjacent regions with some of the major faults, e.g. the Altyn Tagh fault, related to the Indo–Asian collision (adopted from [27]). Colors: black <200 m, light blue ~1000 m, yellow ~2000 m, orange ~3000 m, maroon >4000 m. Dashed box represents approximate area of Fig. 2. Towns: Dl=Delhi, Lh=Lhasa, Ht=Hotan, Gm=Golmud, Dh=Dunhuang, Lz=Lanzhou, Yc=Yinchuan, Ym=Yumen.

(ATF; Fig. 1). Furthermore, these end-member models make predictions about slip rates, magnitudes of displacement, and spatial extent of these and other major structures within and around the Tibetan Plateau.

2. The Altyn Tagh fault

With an along-strike length of >1500 km, the active left-lateral Altyn Tagh fault (ATF) is the largest strike-slip fault in Asia and marks the northern margin of the Tibetan Plateau (Figs. 1 and 2). It is a key structural feature in all tectonic models of Asia; variously cited to support both continuum crustal thickening and plate-like lateral extrusion (Fig. 1; [2,6–11]). Plate-like extrusion models predict high slip rates (>20 mm/yr), and magnitudes for the ATF, whereas continuum thickening deformation requires lower rates (10 mm/yr), and magnitudes of slip on major structures. The former model requires the Altyn Tagh fault to extend beyond the plateau or transfer its slip onto other structures, whereas the latter requires the fault to end at the NE edge of the Tibetan Plateau by transferring slip onto the North Qilian fault (Figs. 1 and 2).

Because of its importance in all models of the Indo-Asian collision, many workers have focused their attention on the ATF. Multiple pre-slip piercing point studies on the eastern and central segments of the ATF have demonstrated a range of common offset of 350–400 km [12–21], and a single pre-Tertiary piercing point on the western ATF suggests 475 ± 70 km of slip at the western end of the fault [21,22]. Piercing point studies, growth strata, paleocurrents, and provenance all suggest that the ATF initiated in the Oligocene [18,23–25]. Current slip rate estimates range from 2–30 mm/yr [26–29], with the most recent value on the eastern-central ATF represented by the 5.6 ± 1.6 mm/yr rate measured using GPS by Zhang et al. [29].

Piecing point studies of Tertiary sedimentary basins on the central and eastern segments of the Altyn Tagh fault have done much to define the mid-Tertiary to Recent slip history of the Altyn Tagh fault. Yue et al. [18,30,31] and Ritts et al., [32] have established multiple piercing points between Tertiary basins and their source terranes that demonstrate large amounts of offset (~310 km) for Oligocene and Early Miocene basins, but small offsets (<65 km) for basins that are mid-Miocene

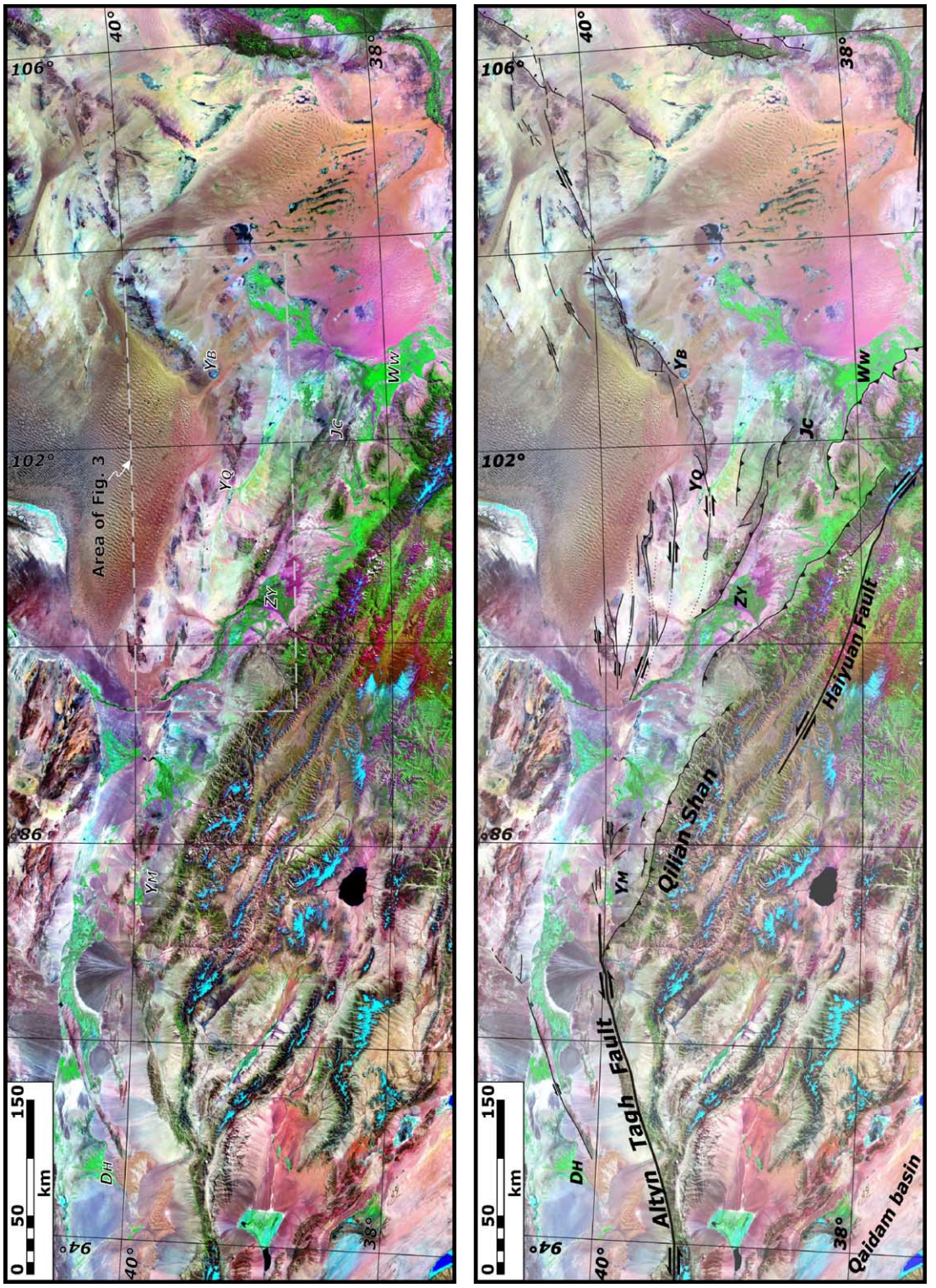

Fig. 2. False color composite Landsat TM image of the northern Tibetan Plateau and Alxa region, China. Interpretation show on lower faded image by the authors. Towns: Dh=Dunhuang, Jc=Jinchang, Zy=Zhangye, Ym=Yumen, Yq=Youqi, Ww=Wuwei. Dashed box on upper image represents approximate area of Fig. 3.

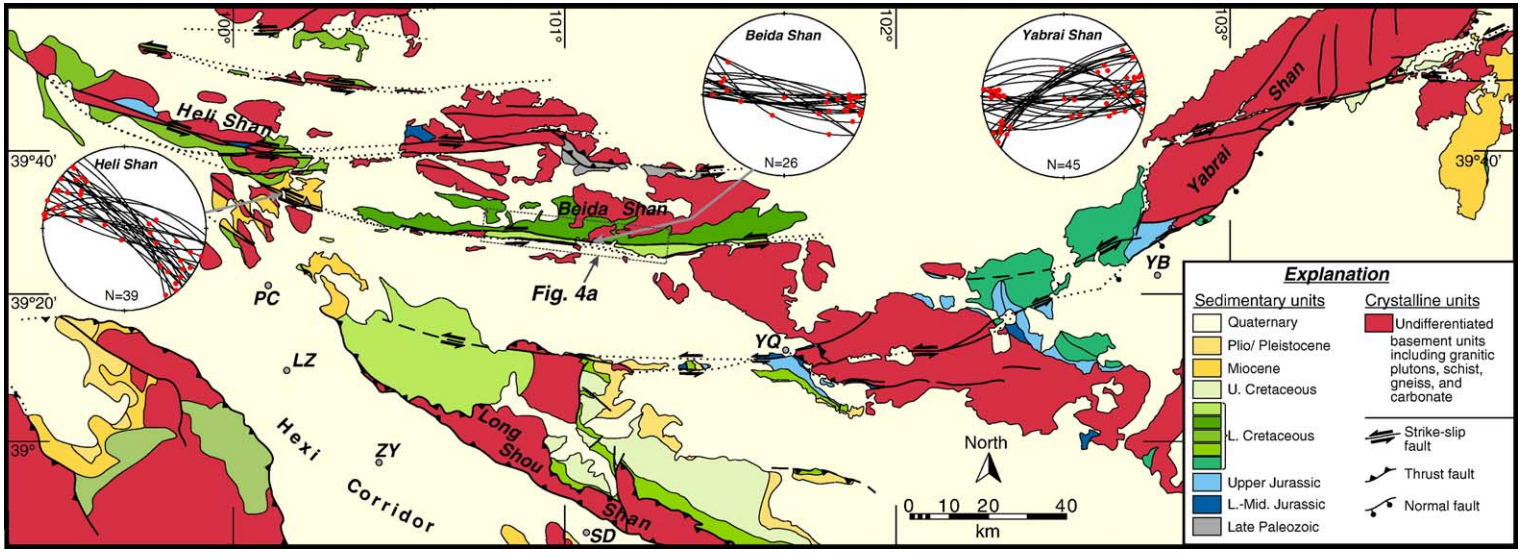

Fig. 3. Simplified tectonic map of the Alxa region based on Summer 2004 fieldwork and Chinese mapping [36,37]. See text for details. Towns: YB=Yabrai, YQ=Alxa Youqi, SD=Shan Dan, ZY=Zhangye, LZ=Linze, PC=Pingchuan. Stereonets are equal area and lower hemisphere. Faults shown in black, red dots represent striae. Data shown from Heli Shan were collected along ~1 km of fault length from fault gouge and many small faults within a 50 m-wide zone where Miocene strata show small (<5 km) of left-lateral offset. Data from the Beida Shan were collected along the northern of the two left-lateral faults that bisect the range from fault gouge and faults in brecciated basement a few 10's of meters north of the fault. Location shown by white star on Fig. 4A. Data shown from Yabrai Shan collected from numerous major structures that bound the range including the mountain front normal fault (down dip to oblique striae) along the southern portion of the range and left-lateral strike-slip faults along the southern flank of the Northern Yabrai Shan.

and younger. These syn-slip piercing points suggest two distinct phases of movement on the ATF: Late Oligocene–Early Miocene fast, high-magnitude slip and post-Early Miocene slow, low-magnitude slip [30,32]. These slip-rate results suggest a coherent model that reconciles the two opposing mechanical models, plate-like crustal extrusion versus continuum deformation [10,30,31]. First, the ATF allowed plate-like lateral extrusion during the Oligocene and Early Miocene with ~310 km of left-lateral displacement and

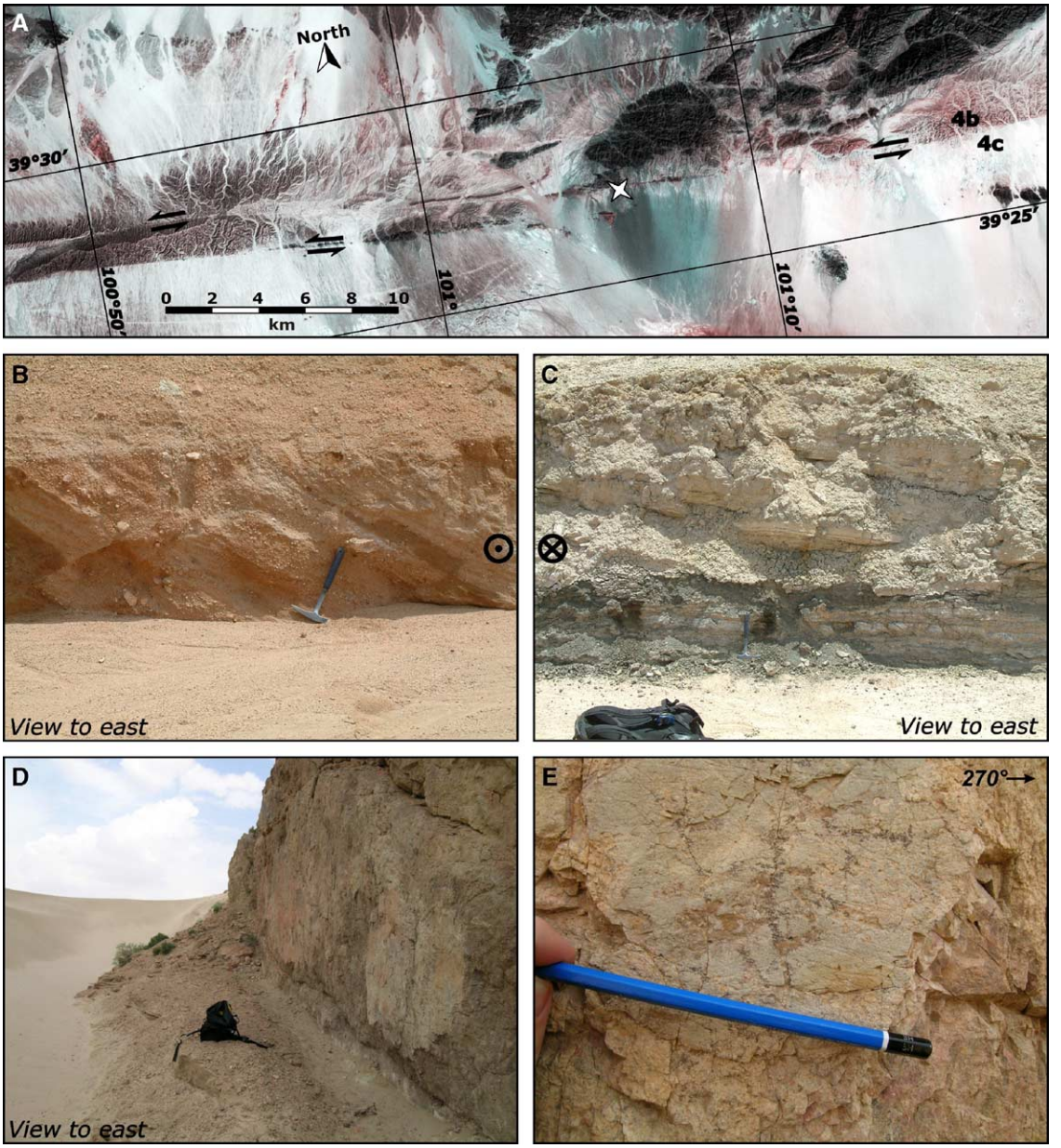

Fig. 4. ASTER image (scene AST_L1B.003:2017827185) of a portion of the Beida Shan illustrating two left-lateral strike-slip faults that bound/bisect the range. Fault and striae data from the Beida Shan shown on Fig. 3 collected from two locations near the white star on the central portion of the image. 4B: Lower Cretaceous strata north of a major left-lateral strike-slip fault in the Beida Shan. Clasts are composed of granite, basalt, dark green and red sandstone and volcaniclastic sandstone. Hammer for scale. 4C: Lower Cretaceous strata south of a major left-lateral strike-slip fault in the Beida Shan. The provenance of this section is distinct from the Lower Cretaceous section to the north of the fault. In addition, this Lower Cretaceous formation is finer grained and contains abundant organic facies. Hammer and backpack for scale. 4D: Well exposed vertical fault plane in the Yabrai Shan. View to the east. Backpack for scale. 4E: Gently west plunging striae from a fault (4D) in the northern Yabrai Shan. Pencil oriented parallel to most prominent set of striae.

slip rates in excess of 20 mm/yr [30]. Second, since the Early Miocene, slip on the ATF has slowed to <10 mm/yr (~the present rate), accumulated only ~65 km of offset, and has accommodated distributed shortening within the northern Tibetan Plateau [30]. Although these fault slip-rate data have been interpreted to suggest a two phase evolution, the mechanism to accommodate extrusion of crustal blocks beyond the Tibetan Plateau remains problematic given three constraints: 1) the ATF is generally considered to end at the NE corner of the Tibetan Plateau, near Yumen (Figs. 1 and 2); 2) the amount of extrusion-related Oligocene–Early Miocene slip on the ATF is suggested to be ~310 km very near the fault's present geomorphic termination near Yumen — beyond the frontal Qilian Shan thrust fault [31]; 3) other structures proposed to accommodate ATF strain near its northeast end (e.g., the Haiyuan fault), do not have the slip magnitudes necessary to have accomplished this [33]. A remaining mechanism for accommodating lateral extrusion, proposed by Yue and Liou [10], suggests transfer of left-lateral slip onto the Alxa–East Mongolia fault system, a system of strike-slip faults posited to extend from the northeast end of the ATF to the Sea of Okhostk. This proposed fault system remains largely a tectonic construct; although supported by sparse geological data from southern Mongolia [34,35] and few seismic studies [10], the existence of Tertiary left-lateral faults remains undocumented northeast of the ATF.

In order to evaluate the presence, distribution, and kinematics of strike-slip faulting beyond the northeast termination of the ATF we completed Landsat/ASTER mapping of the location and lateral continuity of faults combined with geological field studies during 2004 and 2005 within the Alxa block (Figs. 1–4A), immediately east and northeast of the apparent termination of the ATF at the edge of the Tibetan Plateau. Our data demonstrate the presence of multiple large, post-Cretaceous, left-lateral faults that likely have a slip history that is similar to that of the ATF. Specifically, our study documents large (several 10s of km) post-Cretaceous left-lateral slip and minor post-Miocene slip.

3. The Alxa region

The Alxa region in north-central China is located north of the Hexi Corridor and west of the Ordos region (Figs. 1–4A). It contains several mountain ranges that include, from east to west, the Yabrai Shan (Shan= mountain), an unnamed range to the east of Alxa Youqi, the Long Shou Shan, the Beida Shan, and the Heli Shan (Fig. 3). Despite excellent desert exposures and relief that is locally in excess of 1 km, this region remains poorly studied. Fieldwork during Summer 2004 and 2005 suggests that this region has great potential for placing tighter constraints on the tectonic evolution of the ATF and therefore the Tibetan Plateau.

The Alxa region contains rocks ranging in age from Archean to Neogene. Archean–Late Paleozoic basement units are composed of granitic plutons, gneiss, and metasedimentary units (undifferentiated on Fig. 3). Sedimentary sequences include Jurassic sandstone–pebble conglomerate, widespread Lower Cretaceous nonmarine strata, Upper Cretaceous sandstone and conglomerate and Tertiary sandstone and conglomerate. The widespread Lower Cretaceous sedimentary units (Fig. 3; note that all age control is from [36,37]), have been mapped previously as five distinct Lower Cretaceous formations. Lithological distinctions between these formations were confirmed by our fieldwork; Cretaceous strata within fault-bounded panels range from coarse-grained red beds to dark-colored coal-bearing lacustrine and swamp facies with markedly different detrital sediment compositions (Fig. 4B, C).

All of the ranges in the Alxa region are bound or bisected by left-lateral strike-slip faults (Fig. 3). There are at least five major, ~ east–west trending left-lateral fault zones between N39°–40° and E100°–102°; these faults are visible on Landsat and ASTER images and were confirmed with structural observations in the field (Figs. 2–4A, D, E). These faults have variable steep dips (65°–90°) to the north or south, sub-horizontal striae, and fault gouge that varies in thickness from a few centimeters to as much as 9 m (Figs. 3 and 4D, E). The strike of these faults varies from west–northwest in the western Alxa region to east–northeast in eastern areas (Fig. 3). Kinematic indicators, such as tension cracks, steps on fault planes, and s/c-type fabrics in fault gouge document left-lateral slip with a small component of dip-slip (Figs. 3 and 4E). In addition, one of the left-lateral faults in the northern Heli Shan has an impressive fault scarp that offsets a terrace 2–4 m vertically with 8–15 m left-lateral offset of stream channels.

The Beida Shan, in particular, display an exceptional example of left-lateral faulting (Figs. 3 and 4A). The southern margin of the range is controlled by two major ~east–west trending left-lateral strike-slip faults (Figs. 3 and 4A). The northern of the two faults juxtaposes two different Lower Cretaceous sedimentary units for much of its length (dark green vs. light green on Fig. 3). These units have distinct facies, depositional environments, and provenance (Fig. 4B, C). Lower Cretaceous strata on the north side of the fault rest unconformably

on crystalline basement and are dominantly composed of red and green pebble-boulder alluvial fan conglomerate and green sandstone lenses deposited by stream-flow processes (Fig. 4B). Clasts found in Cretaceous strata north of the fault are composed of granite, basalt, dark green and red sandstone, and volcaniclastic sandstone. The Cretaceous strata on the southern side of the fault are finer grained and contain abundant organic facies that are not found north of the fault; lithologies include green and red braided fluvial sandstone, dark gray laminated shale, coal, and lesser pebble–cobble conglomerate (Fig. 4C). In contrast to Cretaceous strata on the northern side of the fault, conglomerate clasts consist of granite and pegmatite with lesser basalt and gabbro; sandstone clasts are not present. The fault between these two Cretaceous sections is marked by gouge and a zone of smaller normal and strike-slip faults several tens of meters wide. This fault strikes 110°, dips steeply to the south, and displays sub-horizontal striae (Fig. 3). An excellent exposure of the northern fault, near the central portion of the range front, juxtaposes basement against Lower Cretaceous sandstone and conglomerate (light green on Fig. 3). All data shown on the Beida Shan stereonet on Fig. 3 were collected from this portion of the northern left-lateral fault in the Beida Shan (Figs. 3 and 4A). Approximately 80 m of basement on the north side of the fault is highly sheared, brecciated, and silicified, and up to 9 m of fault gouge is present, with strong layering that dips steeply (~80°) south (Fig. 3—Beida Shan stereonet). Striae measured in well-layered gouge and on fault surfaces located a few 10's of meters north of the gouge in shattered basement are sub-horizontal (Fig. 3—Beida Shan stereonet). The gouge contains s/c-type fabrics that suggest left-lateral displacement. This sense of slip is supported by tension cracks on fault surfaces in basement just a few meters north of the fault. Quaternary strata are cut by this northern fault, although no prominent geomorphic scarp is present. The Cretaceous section for at least 75 m south of the northern fault is folded about tight, moderate to steeply plunging hinges and contains numerous small faults. Displacement on the north fault could be ≥70 km based upon the along-strike length of the juxtaposition of two distinct Cretaceous sections of the same age and a mis-match in basement units across the faults. The southern of the two faults in the Beida Shan separates a north wall of Lower Cretaceous strata (shown in light green on Fig. 3), from shattered granitic basement to the south. Gouge is also locally present and is up to several meters thick.

The two left-lateral strike-slip faults in the Beida Shan continue west in to the Heli Shan where they cut Miocene conglomerate and sandstone derived from the Qilian Shan thrust belt to the south, which rest unconformably on Cretaceous strata (Fig. 3). Surprisingly, where the faults cut Miocene strata, they do not appear well developed and left-lateral displacement is on the order of <3 km or less based upon the limited separation and offset of recognizable Miocene stratigraphy across the fault (Fig. 5). The Miocene section in the Heli Shan is at least 190 m thick, and the vertical and horizontal separation of Miocene strata (Northeast striking and an average dip of ~15°N) on either side of the left-lateral strike-slip fault, when combined with fault geometry (average orientation: strike ~294°, dip 90° ± 10° and gently plunging striae (Average orientation: 115°, 14°; Fig. 5—stereonet) suggest a strike-slip

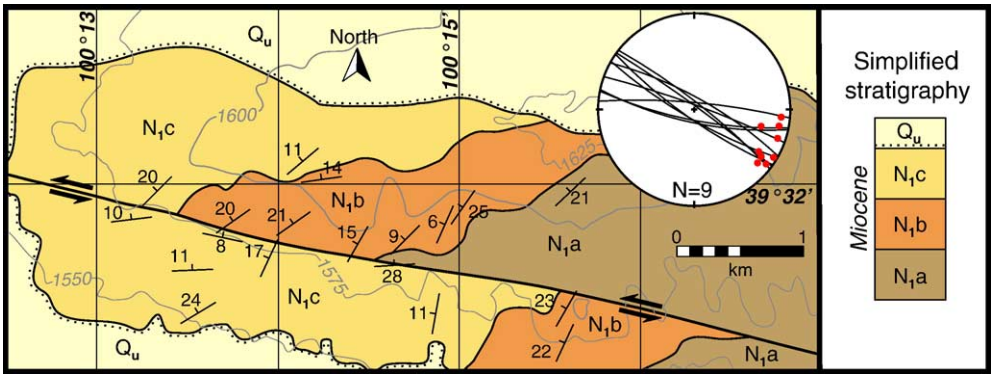

Fig. 5. Geologic map of a small, but important region of the southeastern Heli Shan (location of map shown on Fig. 3 by a small grey triangle ~25 km NNE of Pingchuan-PC). This small area has three distinct Miocene sedimentary units (N_1a, N_1b, N_1c; age control from [36]) which strike ~northeast and have dips to the NW. Truncating these units is a left-lateral strike-slip fault that has ~3 km of post-Miocene displacement. Data shown on the stereonet were collected from three localities along the fault zone in the center portion of the map area. Steps on fault planes and small-scale offsets both support left-lateral displacement. Contour interval=25 m. Topography from SRTM data.

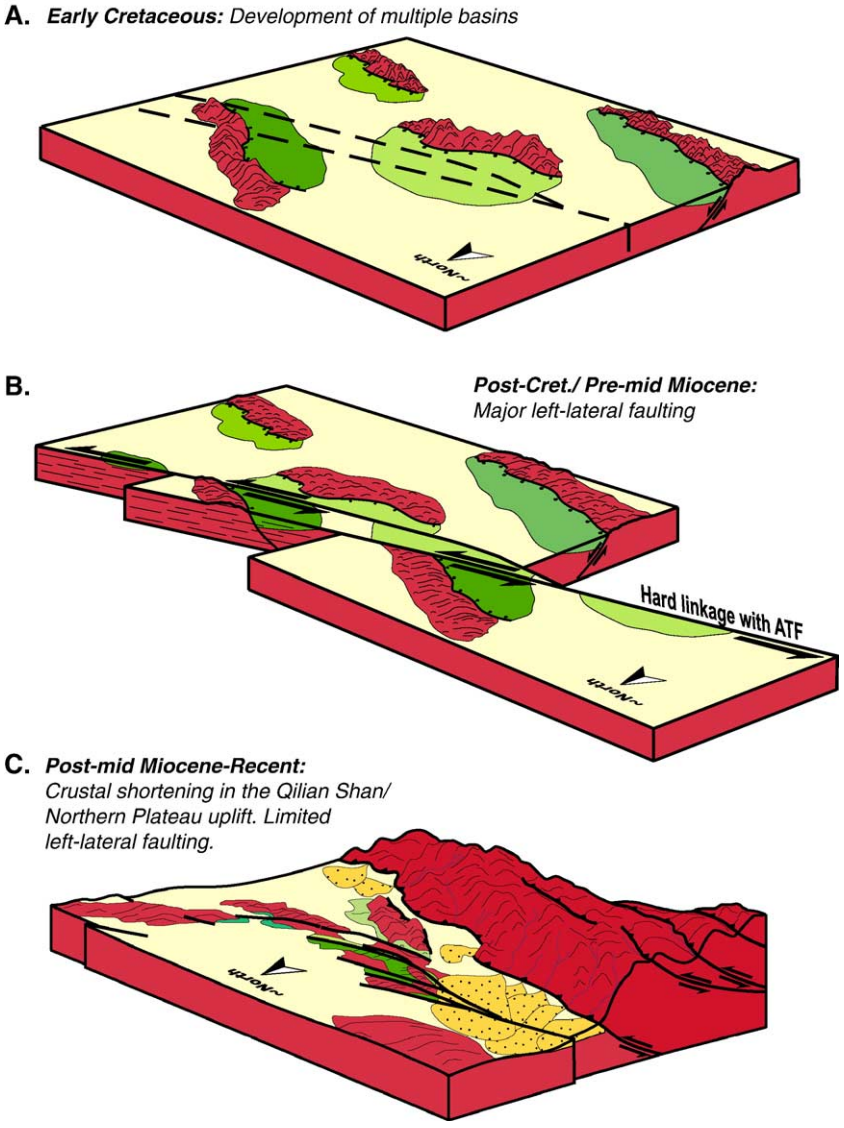

Fig. 6. Schematic block models illustrating the tectonic evolution of the Alxa region. View to the southeast. A. Early Cretaceous basin development (basin location and style undefined). B. Post-Cretaceous/Pre–mid-Miocene major left-lateral faulting. C. Post–mid-Miocene–Recent crustal shortening in the Qilian Shan/northern plateau uplift and limited left-lateral faulting. See text for details. The geometry of the strike-slip faults is unconstrained at depth. Note change in scale between B and C.

displacement of <3 km. All fault and striae data shown from the Heli Shan on Fig. 5 were collected from ~1 km of fault length where Miocene strata are cut and offset. Although it is possible that these left-lateral faults are losing displacement to the west, it is unlikely that they lose 65 km of slip over the 40 km between the Beida Shan and Heli Shan as no structures to absorb this slip, such as thrust faults, have been identified. More likely, these observations imply that post-Cretaceous/pre-Miocene left-lateral slip in the southern Alxa region is large (70+ km) while post-Miocene left-lateral slip has been limited. This slip history for faults in the Heli Shan and Beida Shan is very similar to that described by Yue et al. [30] for the central-eastern ATF. Limited post-Miocene slip is also supported by recent GPS campaigns that show small GPS velocities in the Alxa region with respect to stable Eurasia [29,38] and limited geomorphic evidence of major recent activity.

4. Discussion

The tectonic history of the Alxa region (Fig. 6) described above may have profound implications for strain partitioning related to the Indo-Asian collision

and evolution of the northern Tibetan Plateau. The slip history of left-lateral structures documented in this study is similar to that of the central-eastern ATF as recognized by Yue et al. [18,30] and Ritts et al. [32]. It is possible that the left-lateral faults in the Alxa region represent the pre–mid-Miocene continuation of the ATF system beyond the Tibetan Plateau; a condition required by the large magnitude of slip (at least 310 km, [30–32]) at the present geomorphic termination of the ATF near Yumen, beyond the frontal Qilian thrust fault along the northern margin of the Qilian Shan (Figs. 1 and 2). We suggest that the ATF splayed in to at least five strike-slip faults east of ~98°E longitude (Figs. 2 and 3). This change from a single well-developed structure to multiple, linked, structures may reflect the transition from juxtaposition of disparate basement terranes west of ~98°E (e.g. Tarim from Qaidam/Qilian terranes; [32]) to dissection of the North China block (e.g. the same terrane on both sides of the fault) east of ~98°E. The results from previous studies on the ATF (e.g. [30]) and our data from the Alxa region suggest that pre–mid-Miocene tectonics of northeast Tibet and the Alxa region were dominated by lateral extrusion of crustal blocks on large-scale strike-slip faults that include the ATF as well as structures within the Alxa block — some of which project in to southern Mongolia (Fig. 2; [35]). This system of faults would have continued through eastern Mongolia to the Sea of Okhotsk and linked to the subduction zone along the eastern margin of Eurasia [10,39,40]). We suggest that the Miocene to Recent tectonics of northeast Tibet and the Alxa region include relatively slow rates of slip on the ATF [18,30], crustal shortening and uplift of the northern Plateau in the Qaidam/Qilian Shan region [18,41,42], transfer of some slip from the ATF to the Haiyuan fault [43], and limited left-slip in the Alxa region, which is linked to normal faulting in the eastern Alxa (Yabrai Shan) and formation of the Ordos graben system (Figs. 4–6). The physical connection between faults in the Alxa region and the ATF between Yumen and the edge of Fig. 2, is now mostly covered by Miocene to Recent strata. Reasons for the Miocene change from a lithospheric-scale strike-slip system (extrusion models) to a crustal-scale structure (modern linkage of thrust belts, e.g. [9]) remain enigmatic but may include: 1) a change in convergence rate or angle between India and Asia, 2) passage of a critical mechanical threshold within the Tibetan lithosphere, or 3) a change in the boundary conditions along the Pacific margin, or "free" margin of Eurasia. We favor the third option as there is ample evidence in the geoscience literature for major plate boundary reorganization along the eastern margin of Asia in the Miocene ([40,44–47] and references therein).

5. Conclusions

Our field data and observations from Landsat and ASTER imagery suggest that Alxa region contains at least five left-lateral strike-slip faults (Fig. 3). Based on timing relationships that we have documented in the Beida Shan and Heli Shan (Figs. 3–5), large-scale left-lateral strike-slip faulting ($\geq$70 km of slip) within the Alxa region was temporally restricted to the post-Cretaceous, pre–mid-Miocene (Fig. 6). Post-Miocene to Recent strike-slip faulting in the Alxa region is extremely limited (Figs. 5 and 6). Although total pre-Miocene left-lateral slip on these structures is unknown, it may be much greater than 150 km based upon the juxtaposition of numerous different Lower Cretaceous sedimentary basins (Figs. 3 and 6) and disparate basement units across the structures. These Tertiary structures provide a mechanism to accommodate extrusion of crustal blocks beyond the Tibetan Plateau and must be considered in the Cenozoic tectonic framework of Asia.

Acknowledgements

Financial support of this research comes from Louisiana State University (BJD), NSF/LEQSF 2005-Pfund-02 (BJD), and the National Science Foundation EAR-0207115 (BDR). We would like to thank B. Clark Burchfiel, Richard Phillips, and two anonymous reviewers for reviews of the manuscript. Thanks also to editor van der Hilst for his time and effort.

References

[1] E. Argand, La Tectonique de l'Asie, Int. Geol. Cong. 7 (1924) 171–372.
[2] P. Molnar, P. Tapponnier, Cenozoic tectonics of Asia—effects of a continental collision, Science 189 (1975) 419–426.
[3] M.E. Raymo, W.F. Ruddiman, P.N. Froelich, Influence of late Cenozoic mountain building on ocean geochemical cycles, Geology 16 (1988) 649–653.
[4] W.F. Ruddiman, J.E. Kutzback, Forcing of late cenozoic northern hemisphere climate by plateau uplift in southern Asia and the American west, J. Geophys. Res. 94 (1989) 18409–18427.
[5] P. Molnar, P. England, J. Martinod, Mantle dynamics, uplift of the Tibetan plateau, and the Indian monsoon, Rev. Geophys. 31 (1993) 357–396.
[6] P. Tapponnier, G. Peltzer, A.Y. LeDain, R. Armijo, P. Cobbold, Propagating extrusion tectonics in Asia: new insights from simple experiments with plasticine, Geology 10 (1982) 611–616.

[7] P. England, G. Houseman, Finite strain calculations of continental deformation: II. Comparison with the India–Asia collision zone, J. Geophys. Res. 91 (1986) 3664–3676.
[8] L.H. Royden, B.C. Burchfiel, R.W. King, E. Wang, Z. Chen, F. Shen, Y. Liu, Surface deformation and lower crustal flow in eastern Tibet, Science 276 (1997) 788–790.
[9] B.C. Burchfiel, D. Quidong, P. Molnar, L. Royden, W. Yipeng, Z. Peizhen, Z. Weiqi, Intracrustal detachment zones of continental deformation, Geology 7 (1989) 448–452.
[10] Y.J. Yue, J.G. Liou, Two-stage evolution model for the Altyn Tagh fault, China, Geology 27 (1999) 227.
[11] A. Yin, P.E. Rumelhart, R. Butler, E. Cowgill, T.M. Harrison, D.A. Foster, R.V. Ingersoll, Q. Zhang, X. Zhao, X. Wang, A. Hanson, A. Raza, Tectonic history of the Altyn Tagh fault system in northern Tibet inferred from Cenozoic sedimentation, Geol. Soc. Am. Bull. 114 (2002) 1257–1295.
[12] Z. Che, L. Liu, H. Liu, J. Luo, The constituents of the Altun fault system and genetic characteristics of related Meso-Cenozoic petroleum-bearing basin, Region. Geol. China 17 (1998) 377–384.
[13] X. Ge, J. Liu, Formation and tectonic background of the northern Qilian orogenic belt, Earth Sci. Frontiers 6 (1999) 223–230.
[14] J. Cui, Z. Tang, J. Deng, Y. Yue, Q. Yu, L. Meng, The Altyn Tagh Fault System, Geological Publishing House, Beijing, 1999, 249 pp.
[15] B.D. Ritts, U. Biffi, Magnitude of post-Middle Jurassic (Bajocian) displacement on the Altyn Tagh fault, NW China, Geol. Soc. Am. Bull. 112 (2000) 61–74.
[16] E.R. Sobel, N. Arnaud, M. Jovilet, B.D. Ritts, M. Brunel, Jurassic exhumation history of the Altyn Tagh range, NW China, Geol. Soc. Am. Mem. 194 (2001) 247–267.
[17] J. Yang, Z. Xu, J. Zhang, C. Chu, R. Zhang, J.G. Liou, Tectonic signicance of Caledonian high-pressure rocks in the Qilian–Qaidam–Altun mountains, NW China, Geol. Soc. Am. Mem. 194 (2001) 151–170.
[18] Y. Yue, B.D. Ritts, S.A. Graham, Initiation and long term slip history of the Altyn Tagh fault, Int. Geol. Rev. 43 (2001) 1087–1093.
[19] Y. Yue, J.G. Liou, S.A. Graham, Tectonic correlation of Beishan and Inner Mongolia orogens and its implications for the palinspastic reconstruction of north China, Geol. Soc. Am. Mem. 194 (2001) 101–116.
[20]J J. Zhang, Z. Zhang, Z. Xu, J. Yang, J. Cui, Petrology and geochronology of eclogites from the western segment of the Altyn Tagh, northwestern China, Lithos 56 (2001) 187–206.
[21] G.E. Gehrels, A. Yin, X. Wang, Detrital-zircon geochronology of the northeastern Tibet Plateau, Geol. Soc. Am. Bull. 115 (2003) 881–896.
[22] E. Cowgill, A. Yin, T.M. Harrison, Reconstruction of the Altyn Tagh fault based on U–Pb geochronology: role of back thrusts, mantle sutures, and heterogeneous crustal strength in forming the Tibetan Plateau, JGR 108 (2003).
[23] A.W. Bally, I. Chou, R. Clayton, H.P. Eugster, S. Kidwell, L.D. Meckel, R.T. Ryder, A.B. Watts, A.A. Wilson, Notes on sedimentary basins in China-report of the American sedimentary basins delegation to the People's Republic of China, U.S. Geological Survey Open-File Report 0196-1497 (1986) (108 pp.).
[24] X. Ge, J. Duan, C. Li, H. Yang, Y. Tian, A new recognition of the Altun fault zone and geotectonic pattern of northwest China: IGCP Project 321, Proceedings of First International Symposium on Gondwana Dispersion and Asian Accretion, China University of Geosciences Press, Beijing, 1991, pp. 125–128.
[25] P.E. Rumelhart, A. Yin, R. Butler, D. Richards, X. Wang, X. Zhou, Q. Zhang, Oligocene initiation of deformation of northern Tibet, evidence from the Tarim basin, northwestern China, Geol. Soc. Amer. Abstr. Progr. 29 (1997).
[26] G. Peltzer, P. Tapponnier, R. Amijo, Magnitude of the Quaternary left-lateral displacements along the north edge of Tibet, Science 246 (1989) 1285–1289.
[27] B. Meyer, P. Tapponnier, Y. Gaudemer, G. Peltzer, S. Guo, Z. Chen, Rate of left-lateral movement along the easternmost segment of the Altyn Tagh fault east of 96E (China), Geophys. J. Int. 124 (1996) 29–44.
[28] R. Bendick, R. Bilham, J. Freymueller, K. Larson, Y. Yin, Geodetic evidence for a low-slip rate in the Altyn Tagh fault system, Nature 404 (2000) 69–72.
[29] P. Zhang, Z. Shen, M. Wang, W. Gan, R. Bürgmann, P. Molnar, Q. Wang, Z. Niu, J. Sun, J. Wu, H. Sun, X. You, Continuous deformation of the Tibetan Plateau from global positioning system data, Geology 32 (2004) 809–812.
[30] Y.J. Yue, B.D. Ritts, S. Graham, J. Wooden, G. Gehrels, Z. Zhang, Slowing extrusion tectonics: lowered estimate of post-Early Miocene long-term slip rate for the Altyn Tagh fault, China, Earth Planet. Sci. Lett. 217 (2003) 111–122.
[31] Y.J. Yue, S.A. Graham, S.A., B.D. Ritts, J.L. Wooden, Detrital Zircon Provenance Evidence for Large-Scale Extrusion along the Altyn Tagh Fault, Tectonophysics 406 (2005) 156–178.
[32] B.D. Ritts, Y. Yue, S.A. Graham, Oligocene–Miocene tectonics and sedimentation along the Altyn Tagh fault, northern Tibetan Plateau: analysis of the Xorkol, Subei, and Aksay basins, J. Geol. 112 (2004) 207–229.
[33] B.C. Burchfiel, P. Zhang, Y. Wang, W. Zhang, F. Song, Q. Deng, P. Molnar, L. Royden, Geology of the Haiyuan fault zone, Ningxia-Hui Autonomous Region, China, and its relation to the evolution of the northeastern margin of the Tibetan Plateau, Tectonics 10 (1991) 1091–1110.
[34] C.L. Johnson, Sedimentary Record of Late Mesozoic Extension, Southeast Mongolia: Implications for the Petroleum Potential and Tectonic Evolution of the China–Mongolia Border Region, Stanford University, 2002.
[35] L.E. Webb, C.L. Johnson, Tertiary strike-slip faulting in southeastern Mongolia and implications for Asian tectonics, in review, Earth and Planet. Sci. Lett.
[36] Gansu Bureau of Geol. and Min. Resources, Regional Geology of Gansu Province, Geological Publishing House, Beijing, 1989, 692 pp.
[37] Nei Mongol Bureau of Geol. and Min. Resources, Regional Geology of Nei Mongol Autonomous Region, Geological Publishing House, Beijing, 1989, 725 pp.
[38] Q. Wang, P. Zhang, J. Freymueller, R. Bilham, K. Larson, X. Lai, X. You, Z. Niu, J. Wu, Y. Li, J. Liu, Z. Yang, Q. Chen, Present day crustal deformation in China constrained by Global Positioning System (GPS) measurements, Science 294 (2001) 574–577.
[39] P. Tapponnier, P. Molnar, Active faulting and tectonics in China, J. Geophys. Res. 82 (1977) 2095–2930.
[40] D.M. Worrall, V. Kruglyak, F. Kunst, V. Kuznestsov, Tertiary tectonics of the Sea of Okhotsk, Russia: far-field effects of the India–Eurasia collision, Tectonics 15 (1996) 813–826.
[41] M. Jolivet, M. Brunel, D. Seward, Z. Xu, J. Yang, F. Roger, P. Tapponnier, J. Malavieille, N. Arnaud, C. Wu, Mesozoic and Cenozoic tectonics of the northern edge of the Tibetan Plateau: fission track constraints, Tectonophysics 343 (2001) 111–134.

[42] A.D. George, S.J. Marshallsea, K.-H. Wyrwoll, J. Chen, Y. Lu, Miocene cooling in the northern Qilian Shan, northeastern margin of the Tibetan Plateau, revealed by apatite fission-track and vitrinite reflectance analysis, Geology 29 (2001) 939–942.
[43] P. Tapponnier, Z. Xu, F. Roger, B. Meyer, N. Arnaud, G. Wittlinger, J. Yang, Oblique stepwise rise and growth of the Tibet Plateau, Science 293 (2001) 1671–1677.
[44] G. Kimura, K. Tamaki, Tectonic framework of the Kuril Arc since its initiation 1986a, in: N. Nasu (Ed.), Advances in Earth and Planetary Sciences: Formation of Active Ocean Margins, Terra Sci, Tokyo, 1986, pp. 641–676.
[45] G. Kimura, K. Tamaki, Collision, rotation, and backarc spreading in the region of the Okhotsk and Japan seas, Tectonics 5 (1986) 389–401.
[46] W.P. Schellart, M.W. Jessell, G.S. Lister, Asymmetric deformation in the backarc region of the Kuril arc, northwest Pacific: new insights from analogue modeling, Tectonics 22 (2003), doi:10.1029/2002TC001473.
[47] J.I. Kimura, R.J. Stern, T. Yoshida, Reinitiation of subduction and magmatic responses in SW Japan during Neogene time, Geol. Soc. Amer. Bull. 117 (2005) 969–986.